Chlorophyll dephytylase 1 and chlorophyll synthase: a chlorophyll salvage pathway for the turnover of photosystems I and II

Yao-Pin Lin[1,2,*] (iD), Yu-Yen Shen[2] , Yen-Bin Shiu[2] , Yee-yung Charng[2] (iD) and Bernhard Grimm[1] (iD)

[1]*Institute of Biology/Plant Physiology, Humboldt-Universität zu Berlin, Philippstraße 13 Building 12,10115, Berlin, Germany, and*

[2]*Agricultural Biotechnology Research Center, Academia Sinica, Taipei 11529, Taiwan, ROC*

SUMMARY

Chlorophyll (Chl) is made up of the tetrapyrrole chlorophyllide and phytol, a diterpenoid alcohol. The photosynthetic protein complexes utilize Chl for light harvesting to produce biochemical energy for plant development. However, excess light and adverse environmental conditions facilitate generation of reactive oxygen species, which damage photosystems I and II (PSI and PSII) and induce their turnover. During this process, Chl is released, and is thought to be recycled via dephytylation and rephytylation. We previously demonstrated that Chl recycling in Arabidopsis under heat stress is mediated by the enzymes chlorophyll dephytylase 1 (CLD1) and chlorophyll synthase (CHLG) using *chlg* and *cld1* mutants. Here, we show that the mutants with high CLD1/CHLG ratio, by different combinations of *chlg-1* (a knock-down mutant) and the hyperactive *cld1-1* alleles, develop necrotic leaves when grown under long- and short-day, but not continuous light conditions, owing to the accumulation of chlorophyllide in the dark. Combination of *chlg-1* with *cld1-4* (a knock-out mutant) leads to reduced chlorophyllide accumulation and necrosis. The operation of CLD1 and CHLG as a Chl salvage pathway was also explored in the context of Chl recycling during the turnover of Chl-binding proteins of the two photosystems. CLD1 was found to interact with CHLG and the light-harvesting complex-like proteins OHP1 and LIL3, implying that auxiliary factors are required for this process.

Keywords: chlorophyll salvage, chlorophyll dephytylase 1, chlorophyll synthase, light/dark cycle, photosystem turnover, tetrapyrrole biosynthesis, photosynthesis.

INTRODUCTION

In plants, algae, and cyanobacteria, the pigment chlorophyll (Chl) is indispensable for photosynthesis, which itself sustains most life on Earth. When Chl is assembled into pigment-binding proteins of the two photosynthetic complexes, photosystems I (PSI) and II (PSII), it absorbs solar energy, which drives photosynthetic electron transport and the production of ATP and NADPH. Both molecules are required for the reduction and assimilation of carbon dioxide. The Chl molecule essentially consists of a chlorin ring structure with a central magnesium ion and a hydrophobic phytol tail. The former is excited by irradiation, while the hydrophobic phytol chain helps to anchor Chl to proteins of the photosynthetic complexes embedded in the thylakoid membrane. Both PSI and PSII contain Chl *a* and Chl *b*, although the latter is restricted to the peripheral antenna complexes (Caffarri et al., 2014).

Any sudden impairment of the photosynthetic electron transport chain, as well as fluctuations in environmental conditions, can result in the generation of reactive oxygen species (ROS), such as superoxide and singlet oxygen. These agents can oxidize the photosynthetic core proteins, causing damage that must be promptly repaired to ensure the continuing function of the photosystems. The PSII core protein D1 is particularly vulnerable to overexcitation of Chl and hyperreduction of the initial electron acceptors in PSII. Photodamaged D1 is degraded and subsequently replaced by newly synthesized D1 via the so-called PSII repair cycle (Aro et al., 2005; Järvi et al., 2015). The new D1 protein also requires replenishment with Chl *a*. However, recycling of previously used Chl has not been demonstrated. Thus, new Chl must either be synthesized *de novo* from 5-aminolevulinic acid (ALA), the first committed precursor in the tetrapyrrole biosynthesis (TBS)

pathway (for review, see Tanaka and Tanaka (2007), Brze-zowski et al. (2015), and Grimm (2019)) or be provided by a recently proposed Chl salvage cycle (Lin & Charng, 2021). At present, it is not clear to what extent these two possible modes of Chl supply actually contribute to the provision of Chl for replenishment of newly synthesized D1 and other Chl-binding proteins of both photosystems.

The recently identified Chl dephytylase 1 (CLD1, AT5G38520) suggests a plausible mechanism for Chl *a* turnover via a dephytylation–rephytylation cycle, catalyzed by CLD1 and Chl synthase (CHLG), respectively. CLD1 hydrolyzes Chl *a*, yielding chlorophyllide *a* (Chlide *a*) and a phytol moiety (Lin et al., 2016). Chlide *a* itself serves as the substrate for reformation of Chl *a*, and is esterified with phytyl pyrophosphate (phytyl-PP) or geranylgeranyl pyrophosphate (GG-PP) by CHLG (Rüdiger, 2009) to complete the salvage pathway (Figure 1). During this process, phytyl-PP can be derived either directly from GG-PP through the *de novo* isoprenoid synthesis pathway (Gutbrod et al., 2019) or from the recycled phytol moiety released after Chl hydrolysis (Ischebeck et al., 2006). GG-PP can be reduced to phytyl-PP by geranylgeranyl reductase (GGR) before or after the esterification with Chlide *a* (Tanaka et al., 1999). Continuous Chl turnover, and the reuse of Chlide *a* and phytol, has previously been reported in cyanobacteria and tentatively associated with PSII turnover (Vavilin & Vermaas, 2007).

Our earlier studies identified two EMS-mutagenized Arabidopsis mutants, named *chlg-1* and *cld1-1*, each of which was shown to accumulate Chlide owing to the loss of either the Chlide rephytylation or the Chl dephytylation step in a proposed Chl salvage pathway (Lin et al., 2014, 2016). The *cld1-1* allele encodes a mutant form of CLD1 (CLD1^{G193D}) that is characterized by hyperactive Chl dephytylation. Transgenic plants that overexpressed *cld1-1* (here named *cld1-1*-OE) confirmed the heat-sensitive and Chlide-accumulating nature of the mutant phenotype (Lin et al., 2016).

The *chlg-1* allele was also identified in a screen for thermosensitive mutants. It codes for CHLG^{G217R}, which is unstable and retains only 10–15% of wild-type (WT) CHLG content (Lin et al., 2014). Heat shock (HS) treatment in the dark (HSD) results in Chlide *a* accumulation in *chlg-1* followed by photodynamic cell death in leaves, suggesting that insufficient CHLG activity leads to Chlide accumulation under stress. As *de novo* Chlide *a* synthesis is actively suppressed in the dark, it is evident that excess Chlide can only be derived from Chl dephytylation. In agreement with this assumption, the heat-shocked *chlg-1 cld1-1* double mutant accumulated even higher levels of Chlide *a* and experienced even more dramatic photodamage than either of the parental mutant lines, which confirms that both enzymes contribute equally to the salvage pathway (Figure 1) (Lin et al., 2016). Although such a pathway has been proposed, the physiological details remain unclear. We set out to analyze the mutual interdependency of CLD1 and CHLG and determine the extent to which the Chl salvage pathway contributes to the disassembly and reassembly of the two photosystems.

The turnover and *de novo* synthesis of Chl-binding proteins is accompanied by both synthesis of new Chls and the reuse of previously bound Chls. Newly synthesized Chl-binding proteins are unstable in the absence of Chls (Plumley & Schmidt, 1995) and, conversely, they cannot be degraded without prior removal of Chls (Kusaba et al., 2013). This explains why plants develop a 'stay-green' phenotype when the light-harvesting Chl-binding proteins (LHCPs) of PSI and PSII remain stable during senescence, owing to the inhibition of either Chl dechelation, catalyzed by Mg dechelatase (encoded by *stay-green* [*SGR*]), or conversion of Chl *b* into Chl *a*, catalyzed by Chl *b* reductase (NYC1 and NOL) and 7-hydroxymethyl Chl *a* reductase (HCAR). Such mutant phenotypes, in which both
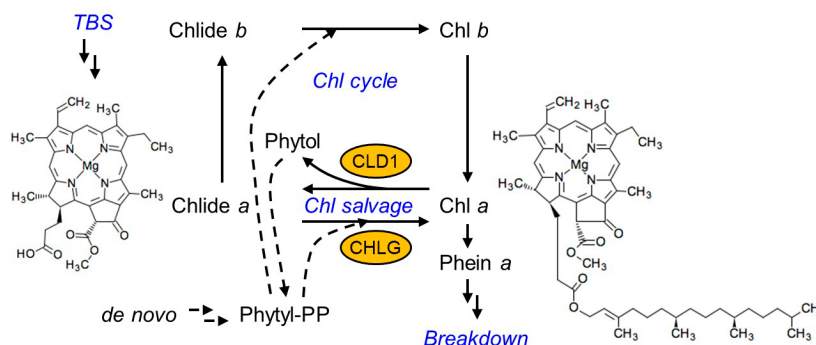

Figure 1. Simplified scheme of the chlorophyll salvage pathway.
Chl *a* is synthesized *de novo* via the tetrapyrrole biosynthesis (TBS) pathway and converted into Chl *b* by esterification of ring B. For Chl turnover, the Chl *a* can be dephytylated to Chlide *a* by the enzyme chlorophyll dephytylase 1 (CLD1) and then rephytylated with *de novo* synthesized or recycled phytyl-pyrophosphate (dashed line) by chlorophyll synthase (CHLG). The molecular structures of Chlide *a* and Chl *a* are derived from the database Kyoto Encyclopedia of Genes and Genomes (https://www.genome.jp/kegg/).

Chl and LHCII contents remain stable in senescent leaves, have been reported in many crops (Kuai et al., 2018; Kusaba et al., 2013; Thomas & Ougham, 2014).

Apart from the LHCPs found in the peripheral antennae of PSI and PSII (light-harvesting complex I [LHCI] and [LHCII], respectively), several other proteins belong to the large family of LHC-like proteins (Wang & Grimm, 2021). These proteins may contain one or several membrane-spanning α-helices. Thus, the plant LHC-like family consists of the one-helix proteins OHP1, OHP2, and ferrochelatase 2 (FeC2), the stress-enhanced proteins SEP1 and SEP2 and the LHC-like proteins LIL3:1 and LIL3:2 with two α-helices each, early light-inducible protein 1 (ELIP1) and ELIP2 with three α-helixes each, and subunit S of photosystem II (PSBS), which has four α-helices (Engelken et al., 2010). These polypeptides have diverse functions associated with Chl metabolism, Chl assembly, light harvesting, and photoprotection (for review, see Andersson et al. (2003), Hutin et al. (2003), Hey et al. (2017), and Hey and Grimm (2018a)). Interestingly, *OHP1*, *SEP1*, and *PSBS*, as well as *CHLG*, show significant co-expression with *CLD1* in Arabidopsis (Obayashi et al., 2017), indicating that these proteins might be functionally associated with the Chl salvage pathway. The cyanobacterial OHP homolog high-light-inducible protein D (HliD) has also been proposed to be involved in Chl recycling during PSII assembly (Knoppová et al., 2014).

We hypothesized that the turnover rate of Chl-binding proteins in photosynthetically active leaf cells depends on the combined action of CLD1 and CHLG in the Chl recycling pathway. Besides exploring the association of CLD1 and CHLG with the Chl salvage cycle, we aimed to examine their impact on the turnover of Chl-containing proteins of the two photosystems. We therefore explored the physiological consequences of altered expression of *CLD1* and *CHLG*, as well as the turnover and stability of core and antenna proteins of the two photosystems in either *CLD1*-overexpressing or -deficient strains, as well as *CHLG* knock-down mutant lines. The results reported here point to the importance of maintenance of an adequate CLD1/CHLG ratio for Chl recycling under adverse as well as normal growth conditions and uncover the dependency of the turnover of Chl-binding proteins of the two photosystems on CLD1 and CHLG.

RESULTS

Light/dark shifts induce photodamage in the mutants *chlg-1* and *cld1-1*

Based on the previous analysis of the heat shock-sensitive mutants *chlg-1* and *cld1-1* (Lin et al., 2014, 2016), we included the *cld1-1 chlg-1* double mutant and the *cld1-1* overexpression line (*cld1-1*-OE) in the present study and grew them in soil at ambient temperature up to 21 days

under short-day (SD) conditions (12 h light/12 h dark), under long-day (LD) conditions (16 h light/8 h dark), or under continuous light (CL). Similar to the previously applied heat treatment, the extended photoperiod caused varying extents of photodamage to the leaves of these lines (Figure 2 and Figure S1). Under SD, growth of *cld1-1* and its OE lines was WT-like, while in both *chlg-1* and *chlg-1 cld1-1* growth was retarded, and the double mutant showed small necrotic lesions on mature leaves. LD lighting proportionately promoted seedling development in all lines, and necrosis was detected in mature leaves of *cld1-1*-OE and *chlg-1 cld1-1*. In contrast, the growth of all mutants was comparable to the WT under CL without obvious necrosis, but leaf pigmentation was reduced in the *chlg-1* and *chlg-1 cld1-1* mutants, which is reflected in the strikingly reduced level of Chl *b* in *chlg-1* and in the total Chl content in the double mutant (Figure 2a,c). Chl fluorescence imaging (Figure 2b) revealed comparable photosynthesis efficiencies in WT and all mutant lines grown in CL.

To see whether darkness is required for triggering necrosis in the mutants, the CL-grown plants were transferred to darkness for 8–24 h and re-exposed to light for 24–48 h. Again, the mutants showed leaf necrosis to variable extents, but damage was always more severe following the extended dark period (Figure 2a and Figure S1a). The *chlg-1 cld1-1* mutant and two representative *cld1-1*-OE lines displayed the most severe cell death phenotype. Although a minor loss of Chl content was observed in all lines during the 24-h dark incubation, the severity of the leaf cell death phenotype in all mutant lines correlated with the increase in Chlide *a* accumulation in the dark (Figure 2c and Figure S1c). At the end of the dark period, the level of protochlorophyllide (Pchlide) was at most twice as high as in the WT. Owing to the much smaller amount of Pchlide (4 pmole mg^{-1} protein) relative to the Chlide levels (up to 200 pmole mg^{-1} protein), Pchlide does not contribute to the photosensitization of the mutants after the dark/light transition. The mutants did not accumulate other tetrapyrrole intermediates, such as Mg protoporphyrin (MgP) and MgP monomethylester (MME), in comparison to WT. After the 24-h dark period and subsequent reillumination, the three most severely affected lines displayed hardly any photosynthetic activity, as determined by PAM Chl fluorescence imaging (Figure 2b). Chlide accumulation in the dark is not attributable to *de novo* TBS via the light-dependent protochlorophyllide oxidoreductase (POR) (Schoefs & Franck, 2003), as also confirmed by the lack of tetrapyrrole intermediates (Figure 2c).

The accumulated Chlide *a* content in darkness correlates with elevated Chl dephytylation by CLD1 and insufficient CHLG activity, a process that was also similarly observed by HS induction (Lin et al., 2014, 2016). Intriguingly, despite the comparable or higher Chlide *a* accumulation in the dark compared to that induced by HS, no dark-induced
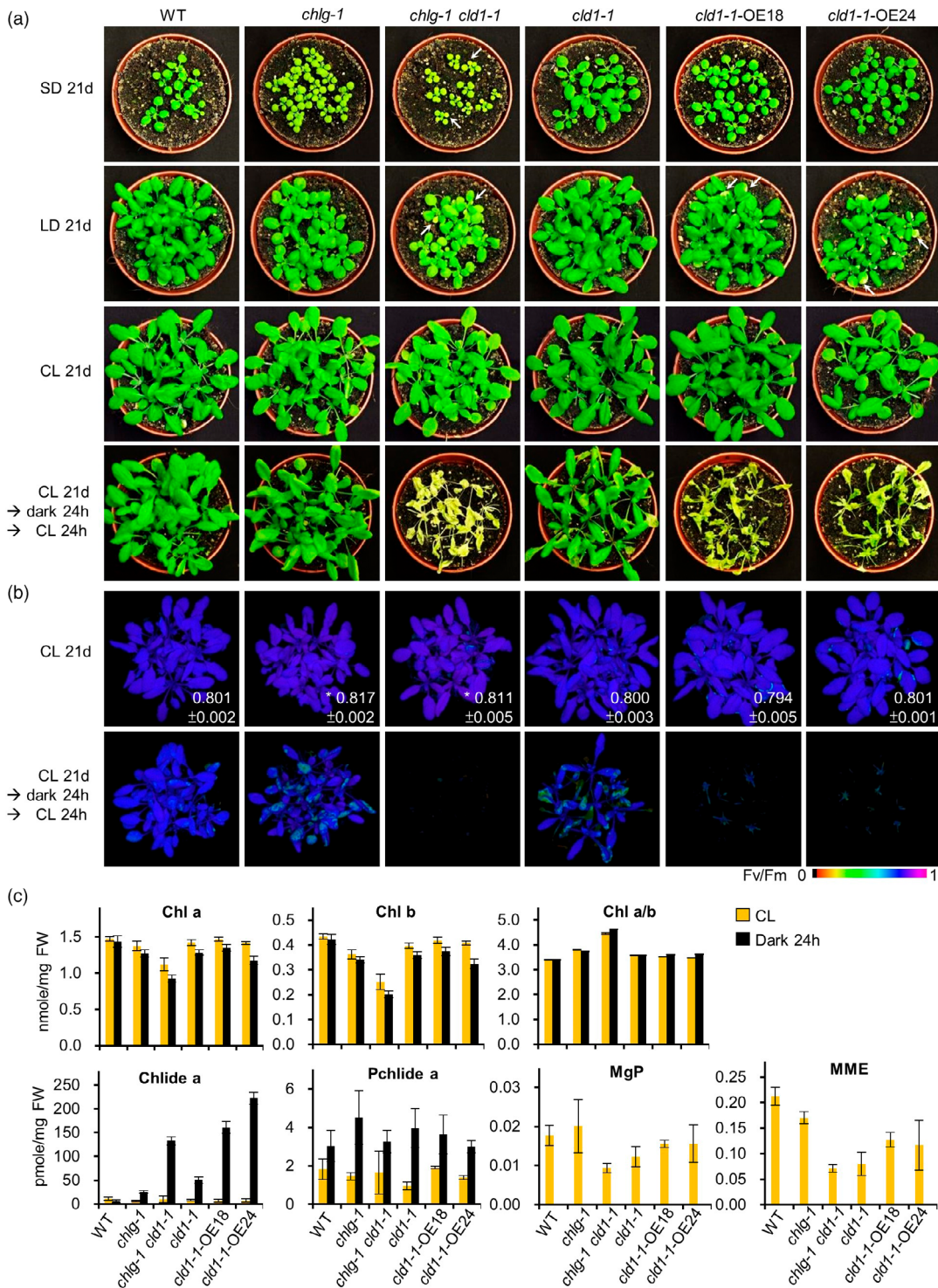
Figure 2. Phenotyping of mutants with varied CLD1 and CHLG activity grown under different lighting conditions (SD: 10 h light; LD: 16 h light; CL: continuous light).

(a) Incidence of leaf necrosis (arrows) in mutants grown under the indicated conditions. (b) Quantification of leaf necrosis (based on the maximum quantum efficiency of PSII) in CL-grown plants before and after dark incubation. The Fv/Fm values determined with an IMAGING-PAM (Walz, https://www.walz.com/) are indicated in false color. Asterisks indicate significant differences between WT and mutant (*t*-test, $P < 0.01$, $n = 5$). (c) Quantification of metabolic intermediates of the TBS pathway (Chlide a, chlorophyllide a; Pchlide a, protochlorophyllide a; MgP, magnesium protoporphyrin; MME, magnesium protoporphyrin monomethylester) and Chls *a* and *b* of CL-grown plants before and after incubation in the dark for 24 h. Data are means (±SD) of three independent experiments. MgP and MME were undetectable following dark incubation.

Chlide *b* was detectable, while HS induces substantial accumulation of Chlide *b* (about 1/15 of Chlide *a*) in these mutants (Lin et al., 2016). These results indicate that the Chl salvage pathway mediated by CLD1 and CHLG actively operates not only under stress, but also under non-stress conditions, and both enzymes are required for the turnover of Chl-binding proteins of the photosynthetic complexes.

We then determined the amount of photosynthetic Chl-binding proteins, CHLG, and CLD1 by immunological analysis of leaf extracts from CL-grown WT and mutant seedlings, either with or without a 24-h dark treatment. Levels of the photosynthetic components D1, PSAL, LHCA1, and LHCB1, as well as CHLG in *cld1-1* or its OE lines, were comparable to those in WT under both light and dark conditions (Figure 3a,c). Similar levels of D1 and PSAL were observed in *chlg-1* and *chlg-1 cld1-1*, but LHCB1 and LHCA1 contents were reduced (LHCB1 by more than LHCA1) compared to WT, indicating that both CLD1 and CHLG coordinately contribute to the control of LHCP levels (Figure 3). The content of CLD1 was not affected in *chlg-1* and *chlg-1 cld1-1*. However, under CL, the amount of CHLG^{G217R} was drastically decreased, although the transcript levels of *chlg-1* were similar to those in WT (Lin et al., 2014). Interestingly, CHLG^{G217R} content declined even further in the dark-treated samples, which points to an additional dark-dependent degradation of mutant CHLG. The significantly reduced stability of CHLG^{G217R} in both light and darkness was quantified in comparison to the WT levels (Figure 3c,d). The T0 samples were harvested at the end of the dark period of SD-grown samples. When SD-grown *chlg-1* and *chlg-1 cld1-1* mutants were exposed to CL, the CHLG^{G217R} content gradually increased to levels similar to those in the CL-grown mutants (Figure 3b,d), i.e., to 10% of WT CHLG levels. As the total Chl content in *chlg-1* reached 90% of the WT level (Figure 2c), low Chl synthase content did not inhibit Chl synthesis strongly under CL. However, the CHLG^{G217R} content becomes insufficient after an extended dark period in *chlg*-1, as the higher Chlide levels indicate. Similarly, *chlg-1 cld1-1* plants show the disruption of the Chl salvage pathway and the enhanced Chl dephytylation in the dark leads to higher Chlide levels (Figure 2 and Figure S1).

The role of CLD1 in the Chl salvage pathway

The *cld1-1* mutant is characterized by enhanced dephytylation and breakdown of Chl. Therefore, we analyzed how loss of CLD1 affects Chl degradation and recycling, as well as the turnover of Chl-containing photosynthetic complexes. *CLD1* knock-out mutants were generated using the *Streptococcus*-derived CRISPR/Cas9 editing system (see Experimental Procedures for details). Among 40 T1 plants showing transgenic antibiotic resistance, two *CLD1* null mutants were isolated and named *cld1-3* and *cld1-4*, respectively. Homozygous progenies of the T2 *CLD1*-

knock-out lines for each mutant were selected by genotyping, which ensured that the transgenic *Cas9* element was lost (Figure S2), thus preventing any further genomic disruption. In the *cld1-3* mutant, nucleotides 113–398 have been lost (see the positions of the single guide RNA [sgRNA] targets in Figure 4a), which also results in a frameshift mutation. The *cld1-4* sequence contains a cytosine insertion at position 399, which leads to a premature stop codon 10 nucleotides downstream. Transcripts of the two *CLD1* mutant alleles were undetectable in both *cld1* mutants, as was the CLD protein, indicating that both mutations are nulls (Figures 4 and 6). The *cld1* knock-out mutants revealed an unspecific immunoreactive band with similar mobility to the WT CLD1. The two *cld1* knock-out mutants grew at WT-like rates in CL and contained similar levels of Chl (Figure 5 and Figure S3). As expected, in contrast to *cld1-1*, the knock-out mutants do not accumulate elevated steady-state levels of Chlide in either light- or dark-exposed plants (Figure 5 and Figure S3b).

When we crossed each *cld1* null mutant with *chlg-1*, the pale green pigmentation of both double mutants resembled that of *chlg-1*, and was confirmed by direct measurements (Figure 5c and Figure S3b). The light-adapted WT and single and double mutants were exposed to two stress conditions: CL-grown plants were exposed to 24 h of darkness or a 1-h exposure to HS (40°C). The *CLD1* knock-out mutant remained WT-like during both treatments, whereas *chlg-1* showed leaf necrosis and an elevated accumulation of Chlide (Figure 5b and Figure S3a). This macroscopic phenotype and the impairments of photosynthetic parameters confirm previous observations (Lin et al., 2014). The double mutant contained 30% less Chlide than *chlg-1* plants, which again indicates that both CLD1 and CHLG contribute to the Chl salvage cycle. Consequently, the double mutant was less severely affected by light exposure during the subsequent recovery period than was *chlg-1*. These observations were also supported by Chl fluorescence images, which revealed that photosynthesis was more severely compromised in *chlg1* than in *chlg1 cld1-4* (Figure 5b and Figure S3a). Thus, loss of CLD1 does not adversely affect the photosynthetic capacity of CL-grown mutant seedlings, and weakens the negative impact of Chlide accumulation caused by deficient CHLG activity.

The impact of the Chl salvage pathway on photosystem turnover

Then, we investigated the connection between the Chl salvage pathway and the turnover of photosynthetic complexes. To assess the effects of an excess or lack of CLD1 activity on the stability and turnover of Chl-binding proteins, we analyzed the contents of PSI and PSII subunits in mutant seedlings exposed to HS or high-light (HL) conditions. Detached leaves of 21-day-old plants grown under CL were incubated at 40°C for 1 h in the dark, which
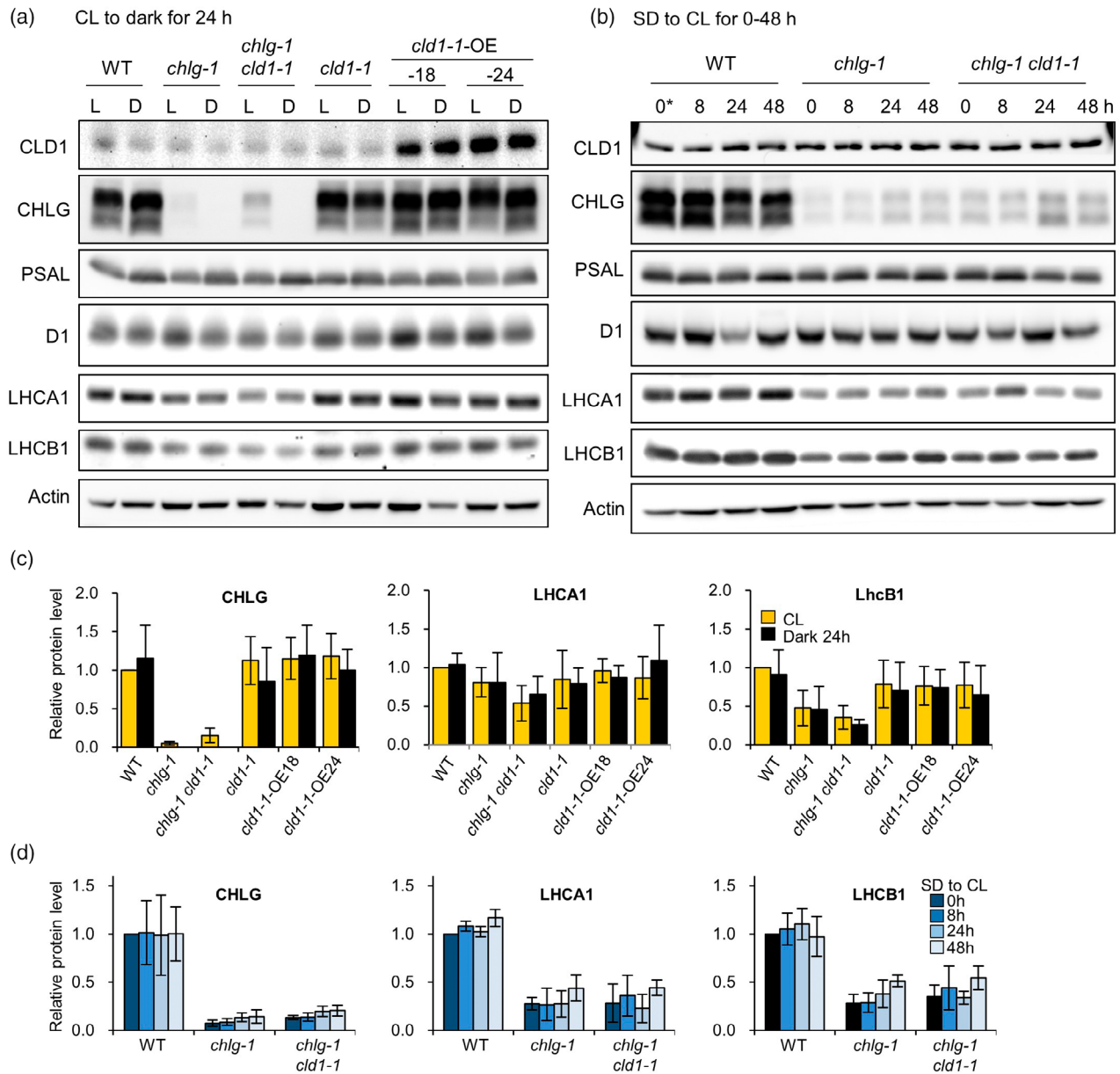
Figure 3. Immunoblot analysis of photosystem subunits.
Total proteins were extracted from (a) 4-week-old CL-grown seedlings that were subsequently incubated in the dark (D) or not (L) and (b) SD-grown seedlings that were subsequently exposed to light for indicated times. The data are quantified (as means ± SD) in panels (c) and (d), based on three independent replicates. The time-point t0* in (b) corresponds to the beginning of light exposure.

suppresses *de novo* D1 synthesis (Figure 6a). In the alternative approach, leaves were incubated in buffered 2 mM lincomycin to inhibit new synthesis of D1 (Figure 6b and Figure S4). Both strategies allowed us to determine rates of D1 degradation.

Compared to the non-stress condition, the CHLG content decreased by 30–40% in all four genotypes analyzed after heat treatment (Figure 6a). This analysis confirmed previously published data (Lin et al., 2014), In contrast, HL treatment had no significant effect on the CHLG level

(Figure 6b). As expected, the HL condition enhanced D1 turnover relative to the HS condition. But, more interestingly, the content of CLD1 influenced the stability of D1 under both HS and HL conditions. CLD1 overaccumulation resulted in a larger pronounced decrease in D1 content relative to WT (Figure 6a and Figure S4a,b). In contrast, levels of the PSI core protein PSAL and LHCA1/LHCB1 did not differ between WT and mutants that were incubated under non-stress or either of the two different stress conditions (Figure 6a,b). Based on these results, we assume that
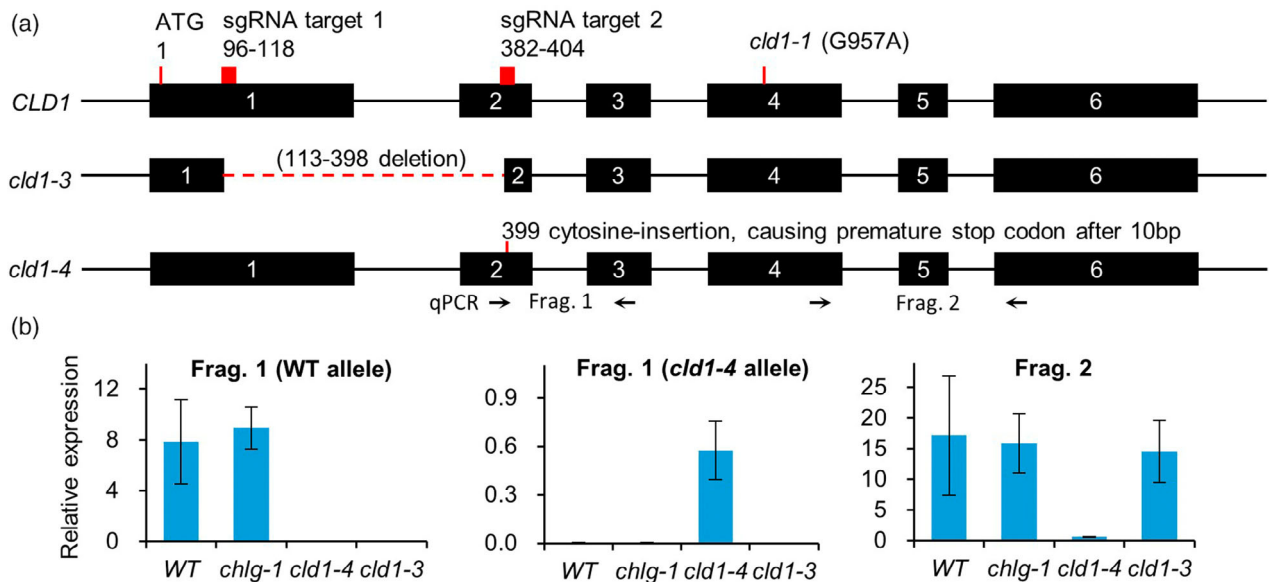
Figure 4. Generation of *CLD1* knock-out lines.
(a) Diagram of the *CLD1* gene and the structures of its alleles. Numbers refer to the amino acid sequences. Black boxes indicate the exons. The two sgRNA target sites used to generate the knock-out lines are indicated. The positions of the mutations in each of the three *CLD1* alleles (*cld1-1* [*G957A*], *cld1-3*, and *cld1-4*) are indicated. (b) Quantitative RT-PCR analysis (qPCR) of WT, *chlg-1*, *cld1-3*, and *cld1-4* transcripts. The relative transcript levels were normalized to that of *SAND*. The bars indicate the means (±SD) of three independent replicates.

CLD1 contributes to D1 turnover by dephytylation of the Chl released from D1. However, although *cld1-3* and *chl1-4* show no clear difference in the content of D1 following heat or high light stress in comparison to WT (Figure 6 and Figure S4b), it is worth pointing out that the CLD1 homologs AT4G36530 and AT5G19850 (Lin et al., 2016) may also redundantly participate in D1 turnover.

We used two-dimensional Blue-Native (BN)-PAGE and SDS-PAGE to further verify the formation and integrity of the photosynthetic complexes in mutants with altered CLD1 and CHLG content after exposure to CL and a 24-h dark incubation (Figure 7). Interestingly, an extra band of an abundant protein complex appears between the PSII dimer and the PSII monomer in samples obtained from both CL-grown and dark-incubated *chlg-1* plants, and to a greater extent in *chlg-1 cld1-1* (Figure 7a,b). This protein complex was not detectable in the CL-grown *cld1-1*-OE line, but became apparent after dark incubation. Presumably, the appearance of this complex is linked either to an insufficiency of CHLG or to an excess of CLD1, as it is observed during growth in the dark and in the light in *chlg-1* and *chlg-1 cld1-1* (Figure 7c).

To determine the nature of this protein complex, its constituents were further fractionated by SDS-PAGE (Figure 7c). Immunodetection of PSAL in this experiment identified the novel band as the PSI core complex. The different PSAL contents in the complexes separated in the first dimension are indicative of the amounts of PSI core and complete complex in each analyzed genotype. Low

amounts of PSAL correspond to less of the PSI core complex in WT, *cld1-4*, and the light-exposed sample of *cld1-1*-OE24, while the increased PSAL content in *chlg-1* and the two double mutants with *chlg-1* reflects higher levels of the PSI core complex (Figure S5). The PSI core complex of *cld1-1*-OE24 accumulates to a greater extent in the dark than under light exposure. In contrast, D1, LHCB1, and LHCA1 – as representatives of the PSII core and the two peripheral antennae, respectively – were found in similar amounts in WT and mutant samples. These data suggest that the PSI core complex accumulates to higher levels when PSI turnover or its *de novo* assembly is perturbed. Interestingly, the loss of *CLD1* in *chlg-1 cld1-4* did not noticeably diminish this complex, once again implicating the other CLD isoforms in the turnover of the two photosystems.

Other proteins that contribute to the Chl salvage pathway

The Chl salvage pathway consisting of CLD1 and CHLG ensures the turnover of PSI and PSII. This process is thought to require assembly and auxiliary factors, either for the incorporation of pigments and cofactors into or their dissociation from the PS proteins (Järvi et al., 2015; Li et al., 2018). To verify the CLD1–CHLG interaction and identify potential interactions between CLD1 and members of the LHC-like protein family, bimolecular fluorescence complementation (BiFC) assays were performed, followed by pull-down assays based on affinity chromatography. CLD1 was fused to the N-terminal portion of yellow fluorescent
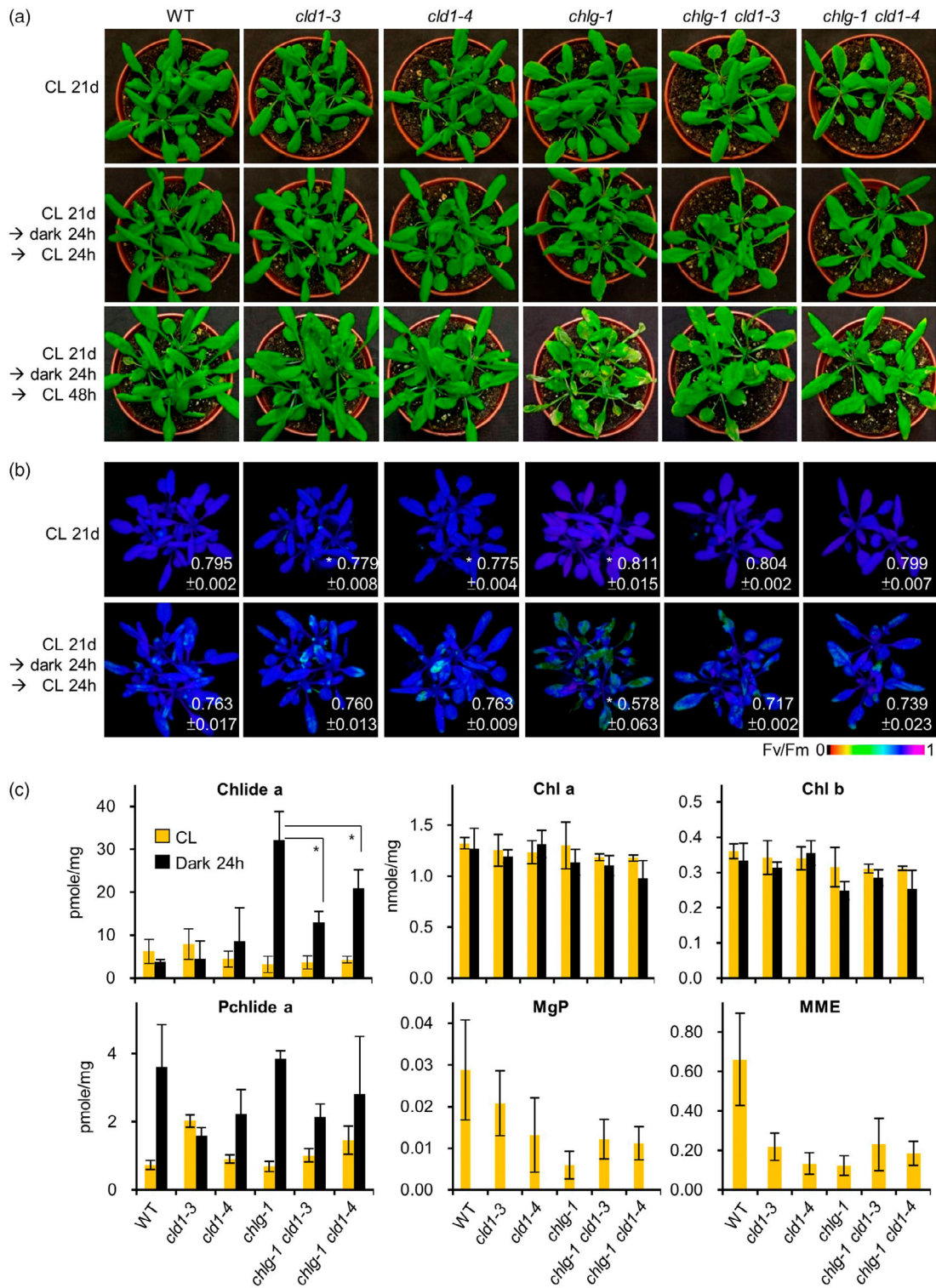
Figure 5. Phenotyping of *chlg-1*, *CLD1* knock-out lines, and double mutants.
(a) Phenotypes of 21-day-old plants grown under CL before and after a 24-h dark incubation following a 2-day exposure to CL. (b) Note the variation in photo-damage among WT and mutant plants, which is quantified in terms of the maximum quantum efficiency of PSII, expressed as Fv/Fm. (c) Quantification of metabolic intermediates of TBS (for abbreviations see Figure 2) and Chls in WT and mutant CL-grown plants before and after 24 h of dark incubation. Data are means (±SD) of three independent experiments. Significant difference with $P < 0.05$ between two compared samples is indicated by *. MgP and MME were undetectable after dark incubation.
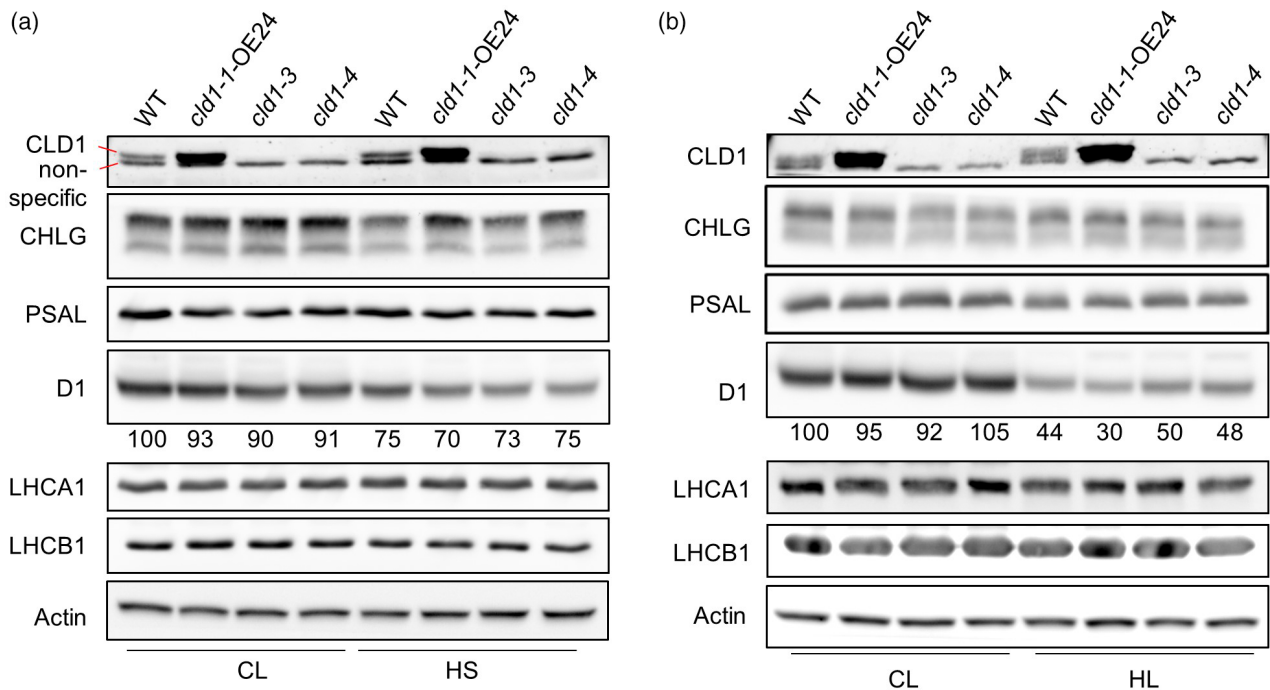
Figure 6. Influence of the activity of the salvage pathway on the turnover of proteins in the two photosystems.
(a) Immunoblot analysis of total proteins extracted from 7-day-old seedlings grown under continuous light (CL) and incubated (or not) for 1 h at 40°C (HS). (b) Immunoblot analysis of total proteins extracted from detached leaves of 21-day-old CL-grown seedlings with or without exposure to high-intensity light (HL). Detached leaves were incubated in 2 mM lincomycin under illumination at 100 (CL) or 500 μmol photons m^{-2} sec^{-1} (HL) for 4 h. The band intensity of D1 protein, normalized to Actin, is directly indicated below the blot. Numbers below the D1 blots represent relative amounts, normalized to Actin, determined by densitometry.

protein (YFP$_N$), and the potential interaction partners were fused to the C-terminal segment of YFP (YFP$_c$). Both fusion proteins were then transiently expressed in *Nicotiana benthamiana* leaves, and reconstitution of the yellow fluorescence indicates that the fusion proteins interact (Figure 8a). Both approaches revealed that histidine-tagged CLD1 (His-CLD1) interacts with CHLG (Figure 8a,c). Subsequently, CLD1 was assayed with the two isoforms of OHP and LIL3. In BIFC assays, yellow fluorescence was observed upon co-expression of CLD1-YFP$_N$ with OHP1-YFC$_c$ or LIL3:2-YFPc, but not with OHP2-YFPc or HCF244-YFPc (HIGH CHLOROPHYLL FLUORESCENCE244, a PSII assembly factor that interacts with OHP2; Hey & Grimm, 2018a), although the fusion proteins were transiently expressed after *Agrobacterium*-mediated transformation of leaves (Figure 8b). To confirm these results, pull-down experiments were performed using His-CLD1, which was expressed in *E. coli*, bound to Ni-NTA agarose beads and incubated with isolated WT thylakoids, as bait. The proteins of the thylakoid membrane fraction were also applied to the affinity column without bound His-CLD1 (negative control). After extensive washing, the bound proteins were eluted with a high concentration of buffered imidazole and fractionated by Tricine-SDS-PAGE (Haider et al., 2012). CLD1 was found also to interact with both

LIL3-1 and OHP-1, while previous reports have excluded CHLG interactions with OHP and LIL3 (Hey et al., 2017; Hey & Grimm, 2018a).

The confirmation of CLD1 interactions with OHP1 and LIL3 prompted us to investigate whether levels of the two LHC-like proteins are modified in *chlg-1* and allelic *cld1* single and double mutants. Total protein extracts from the leaves of 21-day-old CL-grown plants, before and after 24 h dark incubation, were analyzed by immunoblot analysis. Levels of both LIL3:1 and to a lesser extent OHP1 were reduced in samples from dark-incubated WT, *chlg-1*, as well as the *CLD1* hyperactive and knock-out lines (Figure S6). It is hypothesized that the functioning of the Chl salvage pathway requires at least CLD1, CHLG, OHP1, and LIL3 and is more relevant during light exposure. The lower OHP1 and LIL3.1 contents in dark samples could be explained with more instability of the Chl salvage complex or could be due to other varying services of OHP and LIL3 in other pathways during photoperiodic growth.

DISCUSSION

We have described the Chl salvage pathway in Arabidopsis, which consists of the two enzymes CLD1 and CHLG. Their physical interaction was demonstrated by two alternative approaches, BiFC and immunological pull-down
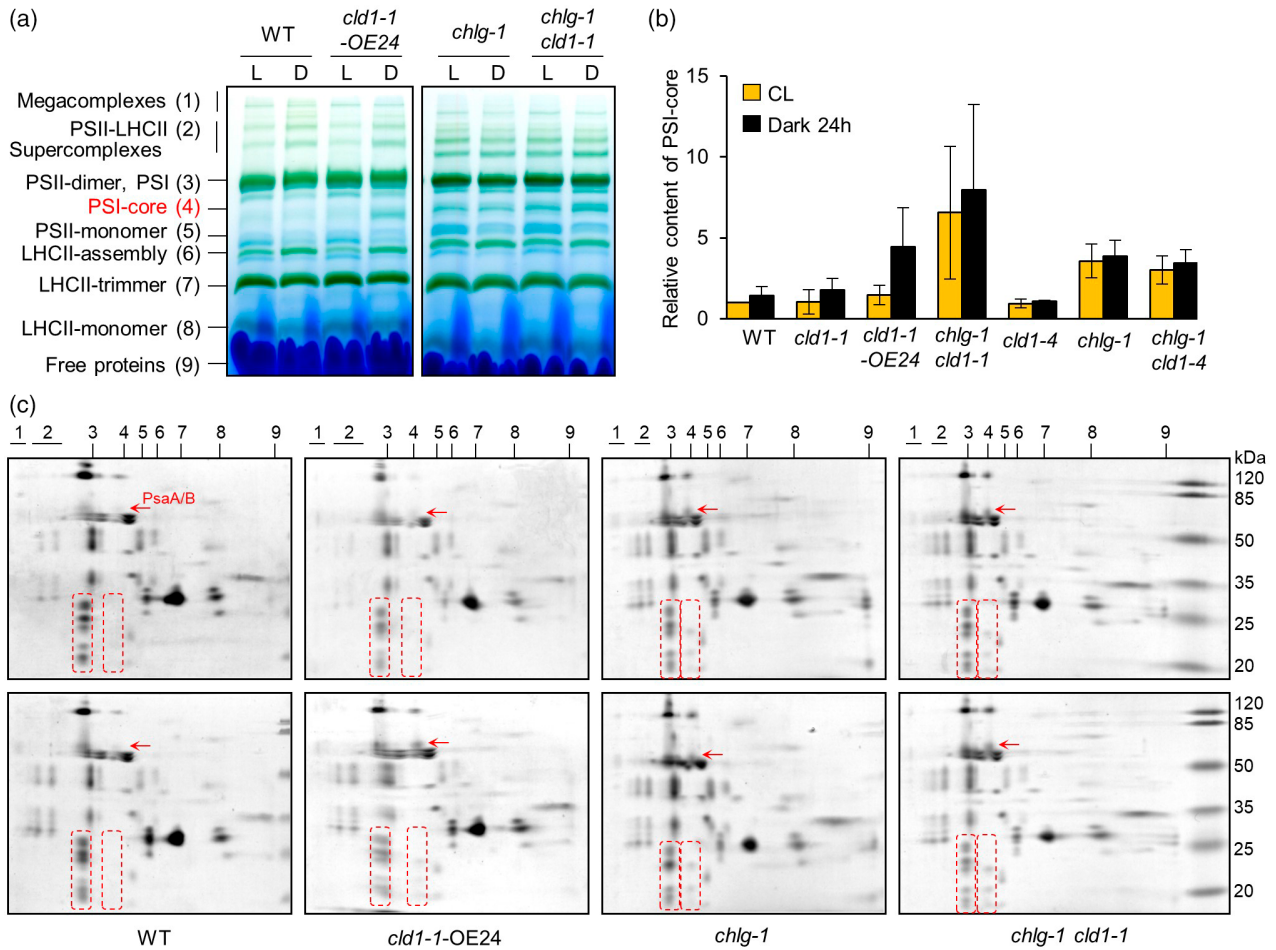
Figure 7. Analysis of photosynthetic complexes and their protein composition during light/dark transitions.
(a) Analyses of pigment–protein complexes in the thylakoid membranes of 21-day-old CL-grown plants exposed (D) or not (L) to a 24-h dark incubation. Thylakoid proteins equal to 10 μg chlorophyll/lane were solubilized with 1% (w/v) DM and analyzed by BN-PAGE. (b) Quantification of the PSI complexes of WT and mutants. The intensity of the respective WT protein band of the light-exposed sample was set to 1. Each histogram depicts the data (means ± SD for three independent replicates). (c) Individual lanes from the gel in (a) were then subjected to denaturing SDS-PAGE in the second dimension. Total proteins were visualized by staining with Coomassie Brilliant Blue. The positions of the PSAA and PSAB proteins are indicated by arrows. The minor proteins in the PSI complex are boxed with dashed lines. Samples that were not subjected to dark incubation are shown in the upper panel, and the lower panel shows the results for dark-treated samples.

assays (Figure 8). These findings suggest that the interaction of the two proteins is a pre-condition for the effective recycling of Chl from proteins that are subjected to proteolysis, as conversion into Chlide *a* (the sole intermediate in the Chl salvage pathway) enables reconstitution of Chls for incorporation into newly synthesized Chl-binding proteins. This salvage pathway thus supplements *de novo* Chl synthesis, which begins with ALA.

The two enzymes act sequentially. CLD1 removes the phytyl substituent from Chl by hydrolysis and the resulting Chlide is then re-esterified with activated phytol or geranylgeraniol. Like the removal of the Mg^{2+} cation by Mg dechelatase (SGR), whose inactivation leads to a stay-green phenotype (Park et al., 2007; Shimoda et al., 2016), it is assumed that Chl dephytylation by CLD1 is a prerequisite for the subsequent proteolysis of Chl-binding proteins.

Besides the physical interaction of CLD1 with CHLG, their functional interrelationship was highlighted when their expression and stability was genetically modified in single and double mutants. Deregulation of the Chl salvage pathway is accompanied by accumulation of Chlide (Figure 2c and Figure S1c). In the *CHLG* knock-down mutant, Chlide accumulation results from insufficient CHLG activity. *CHLG* knock-out mutants are lethal and therefore throw no light on the operation of the salvage pathway (Lin et al., 2014). In addition, we used various *CLD1* alleles either with elevated activity (*cld1-1*) or none at all (*cld1-3*, *cld1-4*) to probe the effects of modified Chl recycling. The CLD1-1 enzyme is more active than the WT protein and leads to accumulation of more Chlide in *cld1-1*, particularly during darkness (Figure 2c). While *cld1-3* and *cld1-4* are both null alleles, these strains still show some dephytylase

Figure 8. Protein–protein interaction assays.
(a) BiFC assays for interaction of CLD1 with CHLG, HCF244, OHP1, OHP2, LIL3-1, and LIL3-2. CLD1 fused to the N-terminal half of YFP was expressed transiently in *Nicotiana benthamiana* leaves, together with each of the potential interaction partners fused to the C-terminal half of YFP. Successful interactions are indicated by yellow fluorescence localized to chloroplasts. Red autofluorescence derives from chlorophyll. (b) Confirmation of the expression of the fusion proteins used in (a) by immunoblot analysis of total proteins extracted from *N. benthamiana* leaves. (c) Immunoprecipitation assays of isolated chloroplasts using CLD1 as the bait and pull-down with an antibody directed against CLD1. * indicates the immune-reacting target proteins fused to the C-terminal half of YFP.
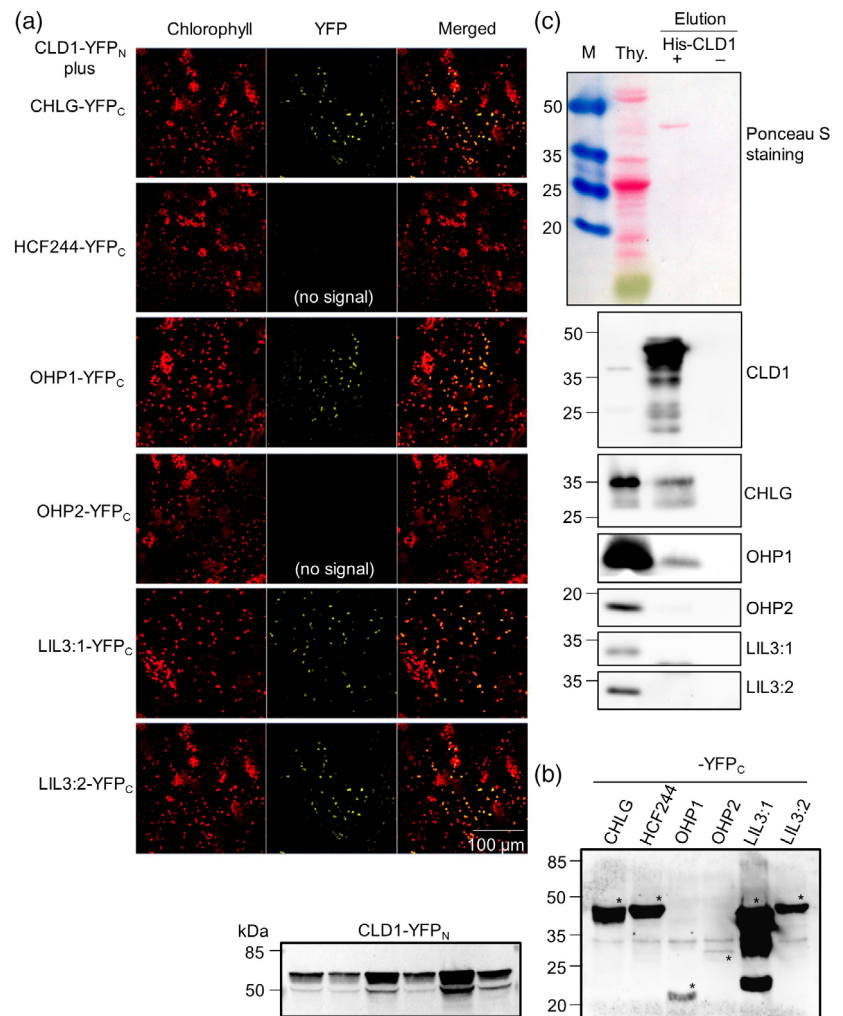
activity, owing to the expression of two other CLD isoforms (encoded by the genes *AT4G36530* and *AT5G19850*). Owing to the lack of CLD1 activity, the *chlg-1 cld1-4* mutant has a lower Chlide content than the *chlg-1* strain (Figure 5c). Thus, excess Chlide accumulation is observed upon either inactivation of CHLG or enhanced CLD1 activity.

Can Chl be synthesized via the Chl salvage pathway in the dark?

Because Pchlide reduction in angiosperms is entirely dependent on light, *de novo* Chl synthesis cannot take place in the dark. This however raises the intriguing question of whether Chl can be synthesized via the salvage pathway in darkness. In principle, the complete Chl salvage pathway could be functional in the dark, as both enzymes could operate independently of light. No Chlide accumulation was detected in single or double mutants for the genes involved in the Chl salvage pathway when plants were grown in the light. But the quantification and kinetics

of Chlide accumulation in dark-grown leaf samples (Figure 2c and Figure S1c) revealed increased Chlide levels in *chlg-1* and *cld1-1* mutants. Clearly, therefore, CLD1 dephytylates Chl and CHLG rephytylates Chlide in the dark, although Chl recycling is assumed to occur in the context of the repair of photodynamically induced damage to Chl-binding proteins during exposure to adverse light levels. The double mutant *chlg-1 cld1-1* accumulates more Chlide in the dark than either *cld1-1* or the WT, and this phenotype becomes even more pronounced in the *cld1-1*-OE lines. These results prompt us to suggest that the low WT Chlide levels are due to dark inactivation of the salvage pathway, either because CLD1 and CHLG inactivate each other by an unknown mechanism or because CHLG still esterifies Chlide to Chl, as long as CLD supplies Chlide in the dark.

Current reports emphasize that the synthesis of D1, and other major subunits of PSI and PSII, takes place only in the light (see review by Sun and Zerges (2015)). But if synthesis of plastid-encoded proteins is confined to the light

period, a Chl salvage cycle in darkness would be meaningless. On the basis of our experiments, CLD1 activity in dark-incubated leaves cannot be excluded. We therefore suggest that, apart from its role in Chl recycling during illumination – when Chlide is recycled to Chl by CHLG – the Chlide produced by CLD1 in darkness can be directed into the Chl catabolic pathway. This would imply differential regulation of Chl catabolism, i.e., senescence-dependent degradation of Chl via the canonical pheophorbide *a* oxygenase (PAO)/phyllobilin pathway and a dark-dependent Chl degradation mechanism mediated by CLD in leaves that still support active photosynthesis and therefore require turnover of Chl-binding proteins. As low amounts of Chl catabolites are always detectable in source leaves (Süssenbacher et al., 2019), products of CLD1 activity can also be directed into Chl degradation. Following this catabolic pathway mediated by CLD1, Chlide *a* is a preferential substrate for SGRL rather than SGR, the predominant initial enzyme in the Chl catabolic pathway through PAO and phyllobilins (Shimoda et al., 2016). SGRL dechelates Chlide to generate phaeophorbide for further degradation of Chl catabolites. This physiological function of SGRL was previously proposed (Bell et al., 2015), and is distinct from the major role of SGR in Chl *a* dechelation during senescence (Shimoda et al., 2016). Transient expression of SGRL in tobacco leaves promotes the degradation of Chl much more effectively in the light than in the dark (Bell et al., 2015). Thus, the potential role of SGRL in the reduction of Chlide in WT, *cld1-1*, and *chlg-1* dark-incubated leaves is worth investigating in the future.

What are preferential target proteins for the dephytylation activity of CLD1?

The reorganization of photosystems following light-mediated damage was initially proposed decades ago (Akoyunoglou & Akoyunoglou, 1985; Argyroudi-Akoyunoglou et al., 1982), but efforts to elucidate further details, including the removal and reassembly of Chl during the turnover of Chl-binding proteins, are still required. The identification of Chl-binding proteins whose Chl is preferentially dephytylated by CLD1 is another intriguing issue. The salvage pathway is likely to be associated with the turnover and recycling of photosynthetic proteins, which includes PS disassembly and assembly and light-dependent *de novo* Chl biosynthesis. Our studies of the salvage pathway enable investigations of the regulatory link between Chl recycling and PSI and PSII turnover.

First insights into the mechanism of disassembly and reassembly of the photosystem complexes were obtained with the *chlg-1* and allelic *cld1* mutants. In comparison to WT, both in the light and the dark, the *chlg-1* mutant was found to contain higher PSI core complex levels (Figure 7). This precursor of the complete PSI complex has been observed before – for example in the Arabidopsis mutants *chaos* and *lhca2* (Otani et al., 2018; Wang & Grimm, 2016) – and it represents an interim step in the assembly of the entire PSI or the disassembly of the PSI antenna. Such extra levels of PSI core complex are more apparent in *chlg-1 cld1-1* and in the dark-incubated *cld1-1*-OE lines (also showing clear correlation with the Chlide *a* surge in the dark (Figure 1c)), indicating the potential involvement of CLD1 activity. Furthermore, higher CLD1 activity in *cld1-1*-OE lines is likely compensated by the action of CHLG in the light. It is not entirely clear whether CHLG actively synthesize Chl in darkness. The post-translational control of CHLG in dark and light is therefore an important topic for future research.

The involvement of the Chl salvage pathway in PSII turnover

PSII turnover, i.e., the molecular mechanism of the controlled degradation and resynthesis of D1 via the PSII repair cycle, has received much attention in recent years (Järvi et al. 2015), but details of the reuse of bound Chls are still lacking. In *CLD1* null mutants, PSII activity was slightly decreased (Figure S3, Fv/Fm is 0.765 in *cld1-4* relative to 0.78 in WT), indicating some influence of CLD1 activity on the efficiency of PSII. Relative to WT, rates of D1 degradation at high temperature and in high light were also slightly enhanced in the *cld1-1*-OE line and reduced in the two *CLD1* knock-out lines (Figure 6). These findings imply that, in D1 turnover, CLD1 may operate redundantly together with the other two CLD isoforms, for which *in vitro* Chl dephytylation activity has recently been demonstrated in cyanobacteria (Takatani et al., 2022). However, in a cyanobacterial mutant which lacks all three Chl dephytylases, proteolysis of D1 proceeds under HL conditions, suggesting that dephytylation by the cyanobacterial CLD homologs plays only a minor role in the degradation of Chl derived from D1 under these conditions in cyanobacteria (Takatani et al., 2022). However, the recovery of PSII activity after HL treatment in the triple mutant takes longer than in WT, pointing to a possible Chl dephytylation/rephytylation, which is performed by other Chl hydrolyzing enzymes. Further experiments with Arabidopsis *cld* triple mutants are necessary to elucidate the role of the Chl salvage pathway in D1 metabolism under normal and photoinhibition conditions.

The chlorophyllase (CLH) isoforms found in Arabidopsis, CLH1 and CLH2, may also belong in this context. CLH was the first Chl dephytylase to be identified – more than a century ago (Willstätter & Stoll, 1911). Although their cytosolic localization and dispensability for Chl breakdown during senescence argue that they are not associated with Chl catabolism in chloroplasts (Hu et al., 2019; Schenk et al., 2007), transfer of CLH1 into the chloroplasts of young leaves was recently proposed, and inhibition of the D1 turnover rate in the *clh1-1 clh2-2* double mutant has been

reported (Tian et al., 2021). Based on these results, faster D1 turnover, greater accumulation of Chlide and pheophorbide, and consequent photodamage could be expected in *CLH* overexpression lines, as has been shown in related experiments (Harpaz-Saad et al., 2007; Kariola et al., 2005). No such assays have been performed in young leaves of CLH1 overexpressors, and indeed the recently reported *CLH1* overexpressors appeared to be more tolerant to light stress (Tian et al., 2021). Further analysis is required to clarify these controversial issues. Finally, *CLD* homologs have been found in cyanobacterial genomes (Schumacher et al., 2022), but no *CLH* genes. Therefore, it is more likely that these CLD isoforms have evolved for Chl salvage during the turnover of the two photosystems, as cyanobacteria use a D1 repair cycle similar to that of plants.

The Chl salvage pathway requires auxiliary factors

The Chl salvage pathway is supported by auxiliary factors. The CLD1–OHP1 interaction is likely to be of crucial importance in the Chl salvage pathway. Previous studies revealed that Hlips (the cyanobacterial homologs of plant OHPs) interact with the photosystem assembly factor Ycf39 and CHLG (Chidgey et al., 2014), while the two OHP1/2 variants in Arabidopsis bind to the HCF244 homolog (Hey & Grimm, 2018a). It was proposed that the OHP1/2- or Hlips-containing complex is localized in close proximity to ribosomes attached to the thylakoid membranes, and contributes to the assembly of Chl into newly synthesized, pigment-binding proteins. Although no interaction of the Arabidopsis CHLG with OHPs could be established (Hey & Grimm, 2018b), it is proposed that OHP1 is required for the integration of Chl into newly translated D1 or other plastid-encoded Chl-binding proteins, and the removal of Chl from photosynthetic complexes and its transfer to CLD1. Thus, the multiple functions of OHPs could include roles in PSII biogenesis and in the synchronized turnover of Chl during PSI disassembly and reassembly.

CLD1 also interacts with LIL3, which associates with POR and GGR (Hey et al., 2017; Tanaka et al., 2010). It has been proposed that LIL3 concurrently binds to both of the latter enzymes to facilitate the provision of stoichiometric amounts of the substrates Chlide and phytyl pyrophosphate for the synthesis of Chl. An interaction of LIL3 with Chl synthase was suggested (Mork-Jansson et al., 2015), but has also been experimentally excluded (Hey et al., 2017). The interaction of CLD1 with LIL3 is however plausible, since CLD1, like POR, supplies Chlide. The formation of a LIL3-mediated complex of these enzymes could promote the channeling of metabolites through these enzymatic steps to ensure the delivery of adequate amounts of substrates via *de novo* Chl synthesis or the Chl salvage pathway. In summary, the likely function of LIL3 in the Chl salvage pathway is to ensure optimal dephytylation of Chl by CLD1 so as to facilitate rephytylation of Chlide by CHLG.

In conclusion, based on the bilateral protein–protein interactions (Figure 8), we propose a model including a protein complex for the Chl recycling, which is composed of at least CLD1, CHLG, OHP1, and LIL3 (Figure 9). We observed diminished contents of CHLG and the two LHC-like proteins OHP and LIL3 in darkness (Figure S6), which indicates that these proteins play more important roles in light than in darkness. Finally, the salvage pathway contributes to photosystem disassembly and assembly, and supports the light-dependent *de novo* Chl biosynthesis by supply of recycled Chl during the turnover of photosynthetic proteins. Our studies of the salvage pathway provide new opportunities to investigate the physiological connection between Chl recycling and PSI and PSII turnover.

EXPERIMENTAL PROCEDURES

Plant materials and growth conditions

Arabidopsis thaliana EMS mutants *chlg-1* and *cld1-1* and its overexpression lines were obtained as described (Lin et al., 2016). Seeds were sterilized, sown on a plate containing 0.8% agar with half-strength Murashige–Skoog medium and 1% sucrose, and imbibed for 2 days at 4°C in the dark prior to incubation at 22°C under the indicated light/dark cycle with 100 μmol photons m^{-2} sec^{-1}. For dark and heat treatment, the plates with seedlings were wrapped in aluminum foil and incubated at 22°C or 40°C for indicated periods. Adult plants grew in soil under CL at 22°C with 70% relative humidity for 21 days prior to 24 h dark treatment.

Analysis of chlorophyll and its intermediates

Total Chl and tetrapyrrole intermediates were extracted from frozen homogenized Arabidopsis seedlings or leaf material with cold extraction buffer (acetone:0.2 N NH_4OH [9:1, v/v]). After vortexing and centrifugation (13 000 *g*, 5 min, 4°C), the supernatant was collected for HPLC analysis. HPLC analysis was performed using reversed-phase chromatography on Agilent HPLC systems, as described previously (Hou et al., 2019). Standards were used for quantification.

Extraction of RNA and quantitative RT-PCR

Total RNA extraction, cDNA preparation, and real-time PCR (RT-PCR) were performed as previously described (Liu et al., 2011; Onate-Sanchez & Vicente-Carbajosa, 2008). Expression of *CLD1* or the mutated allele was analyzed by quantitative RT-PCR with allele-specific primers as listed in Table S1. The expression level was normalized to that of *SAND* (At2g28390) by subtracting the cycle threshold (Ct) value of *SAND* from the Ct value of *CLD1* or its allele.

Generation of *CLD1* knock-out lines by the CRISPR/Cas9 editing system

Transgenic *CLD1* knock-out lines were obtained as described in a previous report (Wang et al., 2015). Briefly, two DNA sequences (TCGCGTCTGTGTTAGAGCCACGG and GGTGCTTCGGATAAGC-CACCTGG) with homology to regions located in *CLD1* exon 1 and exon 2, respectively, were identified by the CRISPR-P 2.0 program (http://crispr.hzau.edu.cn/CRISPR2/) (Liu et al., 2017) as the sgRNA target. The binary vector pHEE401E containing the bacterial *Cas9*
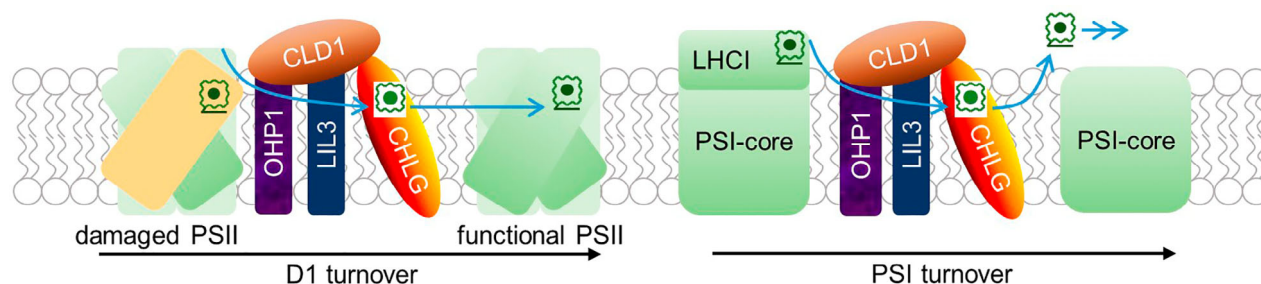
Figure 9. Model of the role of the Chl salvage pathway in photosystem turnover.
During the PSII repair cycle or PSI turnover, the proteins of the Chl salvage, comprising CLD1, CHLG, OHP1, and LIL3, contribute to the dephytylation of Chl derived from the Chl-binding proteins and subsequent rephytylation of Chlide for the reconstitution of Chl (blue route).

gene encoding the endonuclease and the two sgRNA scaffolds targeting the above two *CLD1* sequences was transformed into Arabidopsis accession Col-0. Among 800 progenies of the T1 population, 40 plants were selected based on their antibiotic resistance. The potentially mutated region targeted by the CRISPR/Cas9 system was amplified by PCR with two flanking primers (ATGAGAGCTCTAACATGGACGGC and GGAAGTGGTTCA-GAAACCGA) and sequenced. Eventually, two transgenic plants that lacked detectable CLD1 protein were selected: the *cld1*-3 mutant harboring a cytosine insertion in exon 2, which creates a premature stop codon, and *cld1*-4 containing a deletion located between the sites targeted by the two guide RNAs (Figure 4). The *cld1-2* mutant was mentioned previously in Tian et al. (2021).

Protein extraction and immunoblotting

Total proteins were extracted from Arabidopsis seedlings and leaves and used for immunoblotting as described (Hou et al., 2019). Protein content was quantified using the BCA protein assay kit (Thermo Fisher Scientific, https://www.thermofisher.com/order/catalog/product/23227) and BSA as the standard. For immunoblot analysis, total protein samples were fractionated by SDS-PAGE and Tricine-SDS-PAGE (Haider et al., 2012) and transferred to nitrocellulose membranes for immunodetection by chemiluminescence (Western Lighting Plus-ECL; Bio-Rad, https://www.bio-rad.com/de-de/sku/1705061-clarity-western-ecl-substrate-500-ml?ID=1705061). The polyclonal antisera directed against Arabidopsis CLD1, CHLG, OHP1/2, and LIL3 were generated previously (Hey & Grimm, 2018a; Lin et al., 2014, 2016). The antibodies against PSAL (**AS06 108**), PSBA (**AS05 084**), LhcA1 (**AS01 005**), and LHCB1 (**AS01 004**) were purchased from Agrisera. Chemiluminescent signals were visualized by Clarity Western ECL (Bio-Rad), detected by the ChemoStar Touch Imager (Intas Biopharmaceuticals, Göttingen, Germany), and quantified by ImageJ (National Institutes of Health). Blotted membranes were stained with Ponceau S to verify equal protein loading. Using an old batch of the anti-CLD1 antibody in Figure 3 (from the first purification), only one immune-reacting band of around 38 kDa was detected without a non-specific band (see also Lin et al., 2016). As shown in Figure 6, a new batch of anti-CLD1 antibody generates a non-specific band, which is distinguishable from CLD1 in 8% SDS-PAGE gels (Figure S2b).

Thylakoid isolation and BN-PAGE

Thylakoid membranes were isolated from leaves of 21-day-old plants as described (Järvi et al., 2011). For storage, the isolated thylakoids were resuspended in 25BTH20G buffer (25 mM Bis-Tris, pH 7, and 20% glycerol) and stored at −80°C. The gradient gel with 4–12.5% acrylamide for BN-PAGE was used for the first-dimensional separation of photosynthetic complexes often followed by fractionation under denaturing conditions to resolve their protein compositions. The isolated thylakoids were resuspended in 25BTH20G buffer supplemented with 1% *n*-dodecyl-β-D-maltopyranoside (DDM; BioChemica A0819-0005), incubated on ice for 10 min, and centrifuged at 17 000 *g* for 10 min at 4°C. The supernatant was mixed with 0.1% G-250 running dye and loaded onto gel in a volume equal to 10 μg Chl per lane. Separation of individual proteins by the two-dimensional SDS-PAGE was performed as described (Wang & Grimm, 2016). Following BN-PAGE, single lanes were cut out, denatured in buffer containing 138 mM Tris-HCl, pH 6.8, 6 M urea, 4.3% SDS, 20% glycerol, and 5 mM DTT for 30 min at room temperature, and loaded on a 12% SDS-PAGE gel to separate the individual proteins prior to immunoanalysis. Alternatively, the whole BN-PAGE gel was soaked in the same denaturation buffer as above for 30 min prior to the following immunoblotting assay, as described in the previous paragraph.

BiFC analysis

Amplified *CLD1* and *CHLG* cDNAs (amplified from total cDNA with specific primers carrying attB sites; Table S1) were cloned into pDEST-GW-VYNE/-VYCE vectors (Gehl et al., 2009) via pDON207 using the Gateway system (Thermo Fisher). The vectors pDEST-GW-VYCE containing *OHP1*, *OHP2*, *LIL3:1*, *LIL3:2*, or *HCF244* were generated previously (Hey et al., 2017; Hey & Grimm, 2018a). The desired combinations of recombinant *Agrobacterium tumefaciens* strain GV2260 were infiltrated into *N. benthamiana* leaves and kept in the dark overnight, and the infiltrated leaf areas were analyzed for YFP fluorescence with a confocal microscope (LSM 800; Carl Zeiss, Jena, Germany). Successful transformation and expression of expected protein was confirmed by immunoblotting.

Co-immunoprecipitation analysis

Isolated WT thylakoid membranes (equal to 100 μg Chl) were resuspended in binding buffer (25 mM Tris-HCl, pH 7.8, 150 mM NaCl, 5 mM MgCl₂, 10% [v/v] glycerol, and protease inhibitor cocktail [Roche 11836170001, Germany]). The thylakoids were solubilized with 1% DDM in binding buffer for 10 min on ice and centrifuged at 4°C at 14 000 *g* for 10 min. The supernatant was incubated with 50 μg purified His-CLD1 protein (generated as described in Lin et al., 2016) at 4°C overnight. DDM-solubilized thylakoids without incubation of His-CLD1 were used as a negative control. A 50-μl aliquot of Ni-NTA agarose slurry (Thermo Fisher Scientific) was added to the thylakoid/His-CLD1 mixture, samples were incubated at 4°C for 2 h under gentle shaking and

centrifuged at 4°C at 3000 **g** for 3 min, and the pellet was washed three times using binding buffer containing 20 mM imidazole. Interacting proteins of His-CLD1 were eluted with binding buffer containing 300 mM imidazole, denatured in 2× Laemmli buffer, and analyzed by immunoblotting after separation by Tricine-SDS-PAGE.

ACKNOWLEDGMENTS

AUTHORS CONTRIBUTIONS

Y-PL, Y-YC, and BG designed the research. Y-PL performed the majority of the experiments. Y-YS and Y-BS generated the CLD1-knock-out mutants and confirmed the identity by genotyping. Y-PL, Y-YC, and BG analyzed the data. Y-PL and BG wrote the manuscript with contributions from Y-YC.

CONFLICT OF INTEREST

The authors declare no conflicts of interest.

DATA AVAILABILITY STATEMENT

Data supporting the findings of this work are provided in the main text and the supporting information files. All data and materials used in this study will be available from the corresponding author upon request.

SUPPORTING INFORMATION

Additional Supporting Information may be found in the online version of this article.

Figure S1. Phenotyping of the *CHLG* knock-down mutant (*chlg1-1*) and *CLD1* mutants with enhanced CLD1 activity under light/dark shifts.

Figure S2. Genotyping of *CLD1* knock-out lines.

Figure S3. Phenotypes of *chlg-1* and *chlg1/CLD1* double mutants.

Figure S4. Analysis of the D1 turnover rate under high-temperature or high-light conditions.

Figure S5. Analysis of the protein compositions of photosynthetic complexes during light/dark transition.

Figure S6. Analysis of LHC-like protein contents.

Table S1. List of oligonucleotide primers used in this study.

REFERENCES

Akoyunoglou, A. & Akoyunoglou, G. (1985) Reorganization of thylakoid components during chloroplast development in higher plants after transfer to darkness: changes in photosystem I unit components, and in cytochromes. *Plant Physiology*, **79**, 425–431.

Andersson, U., Heddad, M. & Adamska, I. (2003) Light stress-induced one-helix protein of the chlorophyll a/b-binding family associated with photosystem I. *Plant Physiology*, **132**, 811–820.

Argyroudi-Akoyunoglou, J.H., Akoyunoglou, A., Kalosakas, K. & Akoyunoglou, G. (1982) Reorganization of the photosystem II unit in developing thylakoids of higher plants after transfer to darkness 1: changes in chlorophyll b, light-harvesting chlorophyll protein content, and grana stacking. *Plant Physiology*, **70**, 1242–1248.

Aro, E.-M., Suorsa, M., Rokka, A., Allahverdiyeva, Y., Paakkarinen, V., Saleem, A. *et al.* (2005) Dynamics of photosystem II: a proteomic approach to thylakoid protein complexes. *Journal of Experimental Botany*, **56**, 347–356.

Bell, A., Moreau, C., Chinoy, C., Spanner, R., Dalmais, M., Le Signor, C. *et al.* (2015) SGRL can regulate chlorophyll metabolism and contributes to normal plant growth and development in *Pisum sativum* L. *Plant Molecular Biology*, **89**, 539–558.

Brzezowski, P., Richter, A.S. & Grimm, B. (2015) Regulation and function of tetrapyrrole biosynthesis in plants and algae. *Biochimica et Biophysica Acta (BBA) - Bioenergetics*, **1847**, 968–985.

Caffarri, S., Tibiletti, T., Jennings, R.C. & Santabarbara, S. (2014) A comparison between plant photosystem I and photosystem II architecture and functioning. *Current Protein & Peptide Science*, **15**, 296–331.

Chidgey, J.W., Linhartová, M., Komenda, J., Jackson, P.J., Dickman, M.J., Canniffe, D.P. *et al.* (2014) A cyanobacterial chlorophyll synthase-HliD complex associates with the Ycf39 protein and the YidC/Alb3 insertase. *Plant Cell*, **26**, 1267–1279.

Engelken, J., Brinkmann, H. & Adamska, I. (2010) Taxonomic distribution and origins of the extended LHC (light-harvesting complex) antenna protein superfamily. *BMC Evolutionary Biology*, **10**, 233.

Gehl, C., Waadt, R., Kudla, J., Mendel, R.-R. & Hänsch, R. (2009) New GATE-WAY vectors for high throughput analyses of protein–protein interactions by bimolecular fluorescence complementation. *Molecular Plant*, **2**, 1051–1058.

Grimm, B. (2019) *Metabolism, structure and function of plant tetrapyrroles: introduction, microbial and eukaryotic chlorophyll synthesis and catabolism*. London: Academic Press.

Gutbrod, K., Romer, J. & Dörmann, P. (2019) Phytol metabolism in plants. *Progress in Lipid Research*, **74**, 1–17.

Haider, S.R., Reid, H.J. & Sharp, B.L. (2012) Tricine-SDS-PAGE. In: Kurien, B.T. & Scofield, R.H. (Eds.) *Protein electrophoresis: methods and protocols*. Totowa, NJ: Humana Press, pp. 81–91.

Harpaz-Saad, S., Azoulay, T., Arazi, T., Ben-Yaakov, E., Mett, A., Shiboleth, Y.M., *et al.* (2007) Chlorophyllase is a rate-limiting enzyme in chlorophyll catabolism and is posttranslationally regulated. *Plant Cell*, **19**, 1007–1022.

Hey, D. & Grimm, B. (2018a) ONE-HELIX PROTEIN 2 (OHP2) is required for the stability of OHP1 and assembly factor HCF244 and is functionally linked to PSII biogenesis. *Plant Physiology*, **117**, 1453–1472.

Hey, D. & Grimm, B. (2018b) Requirement of ONE-HELIX PROTEIN 1 (OHP1) in early Arabidopsis seedling development and under high light intensity. *Plant Signaling & Behavior*, **13**, e1550317.

Hey, D., Rothbart, M., Herbst, J., Wang, P., Müller, J., Wittmann, D. *et al.* (2017) LIL3, a light-harvesting complex protein, links terpenoid and tetrapyrrole biosynthesis in *Arabidopsis thaliana*. *Plant Physiology*, **174**, 1037–1050.

Hou, Z., Yang, Y., Hedtke, B. & Grimm, B. (2019) Fluorescence in blue light (FLU) is involved in inactivation and localization of glutamyl-tRNA reductase during light exposure. *The Plant Journal*, **97**, 517–529.

Hu, X., Jia, T., Hörtensteiner, S., Tanaka, A. & Tanaka, R. (2019) Subcellular localization of chlorophyllase2 reveals it is not involved in chlorophyll degradation during senescence in *Arabidopsis thaliana*. *Plant Science*, 110314.

Hutin, C., Nussaume, L., Moise, N., Moya, I., Kloppstech, K. & Havaux, M. (2003) Early light-induced proteins protect Arabidopsis from photooxidative stress. *Proceedings of the National Academy of Sciences of the United States of America*, **100**, 4921–4926.

Ischebeck, T., Zbierzak, A.M., Kanwischer, M. & Dörmann, P. (2006) A salvage pathway for phytol metabolism in Arabidopsis. *The Journal of Biological Chemistry*, **281**, 2470–2477.

Järvi, S., Suorsa, M. & Aro, E.-M. (2015) Photosystem II repair in plant chloroplasts — regulation, assisting proteins and shared components

with photosystem II biogenesis. *Biochimica et Biophysica Acta (BBA) - Bioenergetics*, **1847**, 900–909.

Järvi, S., Suorsa, M., Paakkarinen, V. & Aro, E.M. (2011) Optimized native gel systems for separation of thylakoid protein complexes: novel super- and mega-complexes. *Biochemical Journal*, **439**, 207–214.

Kariola, T., Brader, G., Li, J. & Palva, E.T. (2005) Chlorophyllase 1, a damage control enzyme, affects the balance between defense pathways in plants. *Plant Cell*, **17**, 282–294.

Knoppová, J., Sobotka, R., Tichý, M., Yu, J., Konik, P., Halada, P. *et al.* (2014) Discovery of a chlorophyll binding protein complex involved in the early steps of photosystem II assembly in Synechocystis. *The Plant Cell*, **26**, 1200–1212.

Kuai, B., Chen, J. & Hörtensteiner, S. (2018) The biochemistry and molecular biology of chlorophyll breakdown. *Journal of Experimental Botany*, **69**, 751–767.

Kusaba, M., Tanaka, A. & Tanaka, R. (2013) Stay-green plants: what do they tell us about the molecular mechanism of leaf senescence. *Photosynthesis Research*, **117**, 221–234.

Li, L., Aro, E.-M. & Millar, A.H. (2018) Mechanisms of photodamage and protein turnover in photoinhibition. *Trends in Plant Science*, **23**, 667–676.

Lin, Y.-P. & Charng, Y.-Y. (2021) Chlorophyll dephytylation in chlorophyll metabolism: a simple reaction catalyzed by various enzymes. *Plant Science*, **302**, 110682.

Lin, Y.-P., Lee, T.-Y., Tanaka, A. & Charng, Y.-Y. (2014) Analysis of an Arabidopsis heat-sensitive mutant reveals that chlorophyll synthase is involved in reutilization of chlorophyllide during chlorophyll turnover. *The Plant Journal*, **80**, 14–26.

Lin, Y.-P., Wu, M.-C. & Charng, Y.-Y. (2016) Identification of a chlorophyll dephytylase involved in chlorophyll turnover in Arabidopsis. *Plant Cell*, **28**, 2974–2990.

Liu, H., Ding, Y., Zhou, Y., Jin, W., Xie, K. & Chen, L.-L. (2017) CRISPR-P 2.0: an improved CRISPR-Cas9 tool for genome editing in plants. *Molecular Plant*, **10**, 530–532.

Liu, H.-C., Liao, H.-T. & Charng, Y.-Y. (2011) The role of class A1 heat shock factors (HSFA1s) in response to heat and other stresses in Arabidopsis. *Plant, Cell & Environment*, **34**, 738–751.

Mork-Jansson, A., Bue, A.K., Gargano, D., Furnes, C., Reisinger, V., Arnold, J. *et al.* (2015) Lil3 assembles with proteins regulating chlorophyll synthesis in barley. *PLoS One*, **10**, e0133145.

Obayashi, T., Aoki, Y., Tadaka, S., Kagaya, Y. & Kinoshita, K. (2017) ATTED-II in 2018: a plant Coexpression database based on investigation of the statistical property of the mutual rank index. *Plant and Cell Physiology*, **59**, e3.

Onate-Sanchez, L. & Vicente-Carbajosa, J. (2008) DNA-free RNA isolation protocols for *Arabidopsis thaliana*, including seeds and siliques. *BMC Research Notes*, **1**, 93.

Otani, T., Kato, Y. & Shikanai, T. (2018) Specific substitutions of light-harvesting complex I proteins associated with photosystem I are required for supercomplex formation with chloroplast NADH dehydrogenase-like complex. *The Plant Journal*, **94**, 122–130.

Park, S.-Y., Yu, J.-W., Park, J.-S., Li, J., Yoo, S.-C., Lee, N.-Y. *et al.* (2007) The senescence-induced Staygreen protein regulates chlorophyll degradation. *Plant Cell*, **19**, 1649–1664.

Plumley, G.F. & Schmidt, G.W. (1995) Light-harvesting chlorophyll a/b complexes: interdependent pigment synthesis and protein assembly. *The Plant Cell*, **7**, 689–704.

Rüdiger, W. (2009) Regulation of the late steps of chlorophyll biosynthesis. In: *Tetrapyrroles*. New York: Springer, pp. 263–273.

Schenk, N., Schelbert, S., Kanwischer, M., Goldschmidt, E.E., Dörmann, P. & Hörtensteiner, S. (2007) The chlorophyllases AtCLH1 and AtCLH2 are not essential for senescence-related chlorophyll breakdown in *Arabidopsis thaliana*. *FEBS Letters*, **581**, 5517–5525.

Schoefs, B. & Franck, F. (2003) Protochlorophyllide reduction: mechanisms and evolution. *Photochemistry and Photobiology*, **78**, 543–557.

Schumacher, I., Menghini, D., Ovinnikov, S., Hauenstein, M., Fankhauser, N., Zipfel, C. *et al.* (2022) Evolution of chlorophyll degradation is associated with plant transition to land. *The Plant Journal*, **109**, 1473–1488.

Shimoda, Y., Ito, H. & Tanaka, A. (2016) Arabidopsis STAY-GREEN, Mendel's green cotyledon gene, encodes magnesium-dechelatase. *Plant Cell*, **28**, 2147–2160.

Sun, Y. & Zerges, W. (2015) Translational regulation in chloroplasts for development and homeostasis. *Biochimica et Biophysica Acta (BBA) - Bioenergetics*, **1847**, 809–820.

Süssenbacher, I., Menghini, D., Scherzer, G., Salinger, K., Erhart, T., Moser, S. *et al.* (2019) Cryptic chlorophyll breakdown in non-senescent green *Arabidopsis thaliana* leaves. *Photosynthesis Research*, **142**, 69–85.

Takatani, N., Uenosono, M., Hara, Y., Yamakawa, H., Fujita, Y. & Omata, T. (2022) Chlorophyll and pheophytin Dephytylating enzymes required for efficient repair of PSII in *Synechococcus elongatus* PCC 7942. *Plant and Cell Physiology*, **63**, 410–420.

Tanaka, R., Oster, U., Kruse, E., Rüdiger, W. & Grimm, B. (1999) Reduced activity of geranylgeranyl reductase leads to loss of chlorophyll and tocopherol and to partially geranylgeranylated chlorophyll in transgenic tobacco plants expressing antisense RNA for geranylgeranyl reductase. *Plant Physiology*, **120**, 695–704.

Tanaka, R., Rothbart, M., Oka, S., Takabayashi, A., Takahashi, K., Shibata, M. *et al.* (2010) LIL3, a light-harvesting-like protein, plays an essential role in chlorophyll and tocopherol biosynthesis. *Proceedings of the National Academy of Sciences*, **107**, 16721–16725.

Tanaka, R. & Tanaka, A. (2007) Tetrapyrrole biosynthesis in higher plants. *Annual Review of Plant Biology*, **58**, 321–346.

Thomas, H. & Ougham, H. (2014) The stay-green trait. *Journal of Experimental Botany*, **65**, 3889–3900.

Tian, Y.-N., Zhong, R.-H., Wei, J.-B., Luo, H.-H., Eyal, Y., Jin, H.-L. *et al.* (2021) Arabidopsis CHLOROPHYLLASE 1 protects young leaves from long-term photodamage by facilitating FtsH-mediated D1 degradation in photosystem II repair. *Molecular Plant*, **14**, 1149–1167.

Vavilin, D. & Vermaas, W. (2007) Continuous chlorophyll degradation accompanied by chlorophyllide and phytol reutilization for chlorophyll synthesis in Synechocystis sp. PCC 6803. *Biochimica et Biophysica Acta (BBA) - Bioenergetics*, **1767**, 920–929.

Wang, P. & Grimm, B. (2016) Comparative analysis of light-harvesting antennae and state transition in chlorina and cpSRP mutants. *Plant Physiology*, **172**, 1519–1531.

Wang, P. & Grimm, B. (2021) Connecting chlorophyll metabolism with accumulation of the photosynthetic apparatus. *Trends in Plant Science*, **26**, 484–495.

Wang, Z.-P., Xing, H.-L., Dong, L., Zhang, H.-Y., Han, C.-Y., Wang, X.-C. *et al.* (2015) Egg cell-specific promoter-controlled CRISPR/Cas9 efficiently generates homozygous mutants for multiple target genes in Arabidopsis in a single generation. *Genome Biology*, **16**, 144.

Willstätter, R. & Stoll, A. (1911) Untersuchungen über Chlorophyll. XI. Über chlorophyllase. *Justus Liebigs Annalen der Chemie*, **378**, 18–72.